PLX038: A Long-Acting Topoisomerase I Inhibitor With Robust Antitumor Activity in *ATM*-Deficient Tumors and Potent Synergy With PARP Inhibitors

Anish Thomas[1], Shaun D. Fontaine[2], Morgan E. Diolaiti[3], Parth Desai[1], Rajesh Kumar[1], Nobuyuki Takahashi[1], Linda Sciuto[1], Samantha Nichols[1], Alan Ashworth[3], Felix Y. Feng[3], Gary W. Ashley[2], Minh Nguyen[4], Yves Pommier[1], and Daniel V. Santi[2]

ABSTRACT

Alterations in the *ATM* gene are among the most common somatic and hereditary cancer mutations, and *ATM*-deficient tumors are hypersensitive to DNA-damaging agents. A synthetic lethal combination of DNA-damaging agents and DNA repair inhibitors could have widespread utility in ATM-deficient cancers. However, overlapping normal tissue toxicities from these drug classes have precluded their clinical translation. We investigated PLX038, a releasable polyethylene glycol-conjugate of the topoisomerase I inhibitor SN-38, in *ATM* wild-type and null isogenic xenografts and in a BRCA1-deficient xenograft. PLX038 monotherapy and combination with PARP inhibition potently inhibited the growth of both BRCA1- and ATM-deficient tumors. A patient with an *ATM*-mutated breast cancer treated with PLX038 and the PARP inhibitor rucaparib achieved rapid, symptomatic, and radiographic complete response lasting 12 months. Single-agent PLX038 or PLX038 in combination with DNA damage response inhibitors are novel therapeutic paradigms for patients with *ATM*-loss cancers.

Introduction

Defective DNA repair is a hallmark of cancer and results in genomic instability and accumulation of other genetic abnormalities. Germline mutations of genes involved in DNA repair, such as ataxia telangiectasia mutated (*ATM*), breast cancer (*BRCA*) 1 or 2, and tumor protein 53 (*TP53*) result in markedly increased susceptibility to a variety of cancers. Somatic mutations in these genes are among the most commonly found aberrations in cancer (1, 2). *ATM* plays a central role in DNA damage response (DDR) and is activated by DNA double-strand breaks generated either directly by ionizing radiation or reactive chemicals, or indirectly via the processing of other types of DNA lesions or breakdown of DNA replication forks. ATM phosphorylates and thus activates various proteins that together coordinate the arrest of cell-cycle progression and DNA repair pathways to preserve genome integrity. Mutations in *ATM* are among the most common somatic and hereditary cancer mutations in the general population (3, 4).

Cancers with defective DNA repair mechanisms are commonly more sensitive to treatments that induce DNA damage. ATM loss causes hypersensitivity to various DNA damaging agents including PARP inhibitors (PARPi), topoisomerase I inhibitors (TOP1i), and other S-phase DNA-damaging agents (5, 6). ATM deficiency also increases the dependence of cancer cells on complementary DNA repair mechanisms, specifically repair of replication stress that is incurred by dividing cells. Inhibition of ataxia telangiectasia and Rad3-related (ATR), the regulator of replication stress response, lethally sensitizes cells with defective *ATM* to chemotherapy-induced DNA damage. However, clinical trials of PARPi in *ATM*-deficient tumors have yielded less impressive results compared with those with BRCA1/2 deficiency. The addition of olaparib to paclitaxel failed to improve overall survival over paclitaxel alone in patients with recurrent gastric cancer with low or absent *ATM* expression (7). Also, men with metastatic castration-resistant prostate cancer harboring *ATM* mutations experienced inferior outcomes to PARPi therapy compared with those harboring BRCA1/2 mutations (8). Thus, novel therapeutic approaches are required to leverage the unique sensitivities of *ATM*-deficient cancers.

Irinotecan, or CPT-11, is a clinically important TOP1i widely used in treatment of some of the most common cancers. CPT-11 is metabolically converted to the active metabolite SN-38, which binds tightly to TOP1 cleavage complexes (TOP1cc), which are cytotoxic by their conversion into DNA damage by replication and transcription fork collisions (9). However, the SN-38 formed from CPT-11 has a short half-life of ∼12 hours; without constant exposure to SN-38, the TOP1cc-TOP1i rapidly reverses and the inhibition of TOP1 and DNA damage is terminated. Hence, the duration of DNA damage caused by SN-38 is limited by the short in vivo lifetime of the inhibitor. Nevertheless, in a recent phase I trial of the combination of irinotecan and rucaparib, patients with *ATM*-mutated cancers exhibited most benefit (10). PLX038 is a long-acting prodrug of SN-38 composed of a 40 kDa PEG attached to four SN-38 moieties by linkers that slowly cleave to release SN-38 (see compound **16D** in ref. 11). The prodrug and released SN-38 have $t_{1/2}$ values of about 5 days in humans, about 10-fold longer than the SN-38 released from CPT-11. Also, the small 15 nm nanomolecule readily penetrates large pores of tumor vasculature, and accumulates and is retained in the tumor microenvironment for long periods through the enhanced permeability and retention effect (12). Hence, PLX038 should provide a prolonged duration of DNA damage to achieve synthetic lethality of DNA repair deficient or inhibited tumors.

Because of the well-established synergy of TOP1i with PARPi (13, 14), and the hypersensitivity of *ATM*-deficient cells to both TOP1 and PARP inhibition (5, 6), we hypothesized that the combination of both agents

[1]NCI, NIH. [2]ProLynx, San Francisco, California. [3]UCSF Helen Diller Family Comprehensive Cancer Center, San Francisco, California. [4]Clovis Oncology, San Francisco, California.

Corresponding Authors: Daniel V. Santi, Research and Development, ProLynx LLC, 455 Mission Bay Blvd S, San Francisco, CA, 94158. E-mail: daniel.v.santi@prolynxinc.com; and Anish Thomas, anish.thomas@nih.gov

Mol Cancer Ther 2022;21:1722–8

doi: 10.1158/1535-7163.MCT-22-0217

might be particularly effective in tumors with *ATM* loss. However, thus far, the combination of TOP1 and PARPi have been unsuccessful because of overlapping myelosuppression from both drug classes. A potential approach for achieving safe combinations of DNA damaging agents and DDR inhibitors (DDRi) involves a "gapped-schedule" (15). Here, a tumor-targeted DNA-damaging chemotherapy is first administered that passively accumulates in the tumor, followed by an interval, or gap, that allows for systemic but not tumor elimination of the agent; then, during a critical time window when the DNA-damaging agent is present in the tumor but is low in normal tissues the DDRi is administered.

In this work, in mouse models, we demonstrate synergy of PLX038 with PARP inhibition administered either concurrently or by a gap schedule; this provides a preclinical rationale for a clinical trial of the combination. We next show sensitivity of an *ATM*-deficient tumor to single-agent PLX038 and high synergy upon combination with a PARPi. Finally, we describe a remarkable complete response to the combination of PLX038 with the PARPi rucaparib in a patient with *ATM*-deficient breast cancer.

Materials and Methods

Materials

PLX038 (**16D** in ref. 11) and PLX038A (**1B** in ref. 16) was prepared according to published procedures. Clinical-grade PLX038 was from ProLynx, Inc. Talazoparib was purchased from MedKoo (Catalog No. 204710) and used as received.

Xenograft studies

Dosing solutions of PLX038A were prepared in isotonic acetate, pH 5, to contain 0.19 to 6 mmol/L of SN-38 to deliver 1.9 to 60 μmol/kg. SN-38 content was verified by A_{363nm} ($\varepsilon = 22{,}500\ M^{-1}\ cm^{-1}$). Solutions of TLZ were prepared in 10% dimethylacetamide/6% Solutol/84% PBS at pH 7.4 to contain 50 to 100 μmol/L TLZ to deliver 0.2 to 0.4 μmol/kg. TLZ content was verified by A_{310nm} ($\varepsilon = 9872\ M^{-1}\ cm^{-1}$).

Animal studies were carried out as described previously (16) and in accordance with and approval from the UCSF Institutional Animal Care and Use Committee. MX-1 cells were obtained from the NCI. MX-1 xenografts were established in female nu/nu nude mice as reported previously (16, 17). When tumors reached 170 mm^3, mice received a single intraperitoneal dose of vehicle, a single intraperitoneal dose of PLX038A (15 μmol/kg), a daily oral gavage of free TLZ (0.4 μmol/kg), or a combination of PLX038A (15 μmol/kg) and daily oral TLZ (0.4 μmol/kg) starting on either day 0 (same day as PLX038A dosing) or day 4.

The 22Rv1 *ATM* KO, derived via CRISPR/Cas9 genome editing, harbors a biallelic 33-nucleotide insertion in *ATM*, resulting in a premature stop codon; the 22Rv1 *ATM* KO lacked detectable *ATM* protein by immunoblotting and IHC (18). To establish 22Rv1 xenografts, 10^{-7} cells [in 100 μL of 1:1 PBS:Matrigel (BD Biosciences, 356237)] were subcutaneously injected into the flank of male NSG mice. When tumors reached ∼125 mm, mice received a single intraperitoneal dose of PLX038A (3.75–60 μmol/kg) and/or daily oral gavage of free TLZ (0.2–0.4 μmol/kg/day) for 21 days. Tumor volumes measured by caliper [$0.5 \times (\text{length} \times \text{width}^2)$] and body weights were determined twice weekly. Event-free survival analyses were performed using Prism 8.0 with an event defined as a four-fold increase in tumor volume from the day of treatment.

In vivo statistical methods

To compare treatment and control groups in xenograft studies, the AUC values for a stated time period (usually ∼ 1 month) were calculated for growth curves of each individual in each group, then two-tailed *t* tests were used to assess statistical significance between groups. The log-rank (Mantel–Cox) test was used for analysis of the time to reach four-fold initial tumor volume. Tests were done on GraphPad Prism software (version 9.3.1). Significance is indicated as follows: ns (not significant; *, $P < 0.05$; **, $P < 0.01$; ***, $P < 0.001$).

Clinical studies

A synopsis of the clinical trial design of PLX038 and rucaparib referred to in this work may be found at Clinicaltrials.gov using the identifier NCT04209595. The ongoing study is being conducted in accordance with International Conference on Harmonisation Good Clinical Practice (ICH GCP) and the following: U.S. Code of Federal Regulations (CFR) applicable to clinical studies (45 CFR Part 46, 21 CFR Part 50, 21 CFR Part 56, 21 CFR Part 312, and/or 21 CFR Part 812). The studies were performed with the approval of the NIH Institutional Review Board and with the written consent from patients.

The primary objective of the trial is to identify the MTD of PLX038 in combination with the PARPi rucaparib. This is an open label phase I/II trial, accruing initially one cohort to determine MTD of combined treatment of PLX038 and rucaparib (phase I); and to examine safety and efficacy of the PLX038 in combination with rucaparib in subjects with small cell cancers (phase II). Up to five dose levels of combined treatment of PLX038 and rucaparib will be tested in phase I. PLX038 will be administered on day 1 and rucaparib after a gap of 3 days till day 19, in 21-day cycles. Once an MTD of combined treatment has been determined, up to 35 subjects will be evaluated at MTD in phase II. Administration of PLX038 will be every 3 weeks by intravenous infusion starting on day 1 of cycle 1. Rucaparib will be administered on days 3 or 5 to day 19 of a 21-day cycle starting at 300 mg orally twice daily. Treatment with PLX038 and rucaparib will continue until participant meets off-treatment criteria which include disease progression and or toxicity.

Data availability

The data generated in this study are available upon reasonable request from the corresponding author.

Results

Preclinical studies

Optimal efficacy of a macromolecular prodrug requires balancing the rate of drug release with the rate of prodrug elimination. Because macromolecules have different elimination rates in different species, a prodrug optimal for one species will likely not be for another. In mice, renal elimination of PLX038 has a $t_{1/2,1}$ of only ∼1 day compared with about 6 days in humans, and rapid clearance of PLX038 occurs before significant SN-38 is released. In response to this problem, a faster cleaving linker was incorporated to create the analogous PLX038A and harmonize the rate of drug release with prodrug elimination for use in murine models (compound **1B** in ref. 16). Single doses of PLX038A induced >50% volume regressions in 25 of 32 xenograft tumors tested, and correlated with sensitivity to irinotecan (19). PLX038A also showed remarkable activity in the BRCA1-deficient MX-1 model, where a single dose caused rapid tumor shrinkage and eight of nine tumors had maintained complete responses for 60 to 150 days (16).

PLX038A shows synergy with PARPi when administered concurrently or in a "gap-schedule." **Figure 1A** and **B** shows tumor growth of BRCA1-deficient MX-1 xenografts treated with a single low dose of 15 μmol/kg PLX038, daily doses of 0.4 μmol/kg talazoparib (TLZ), and

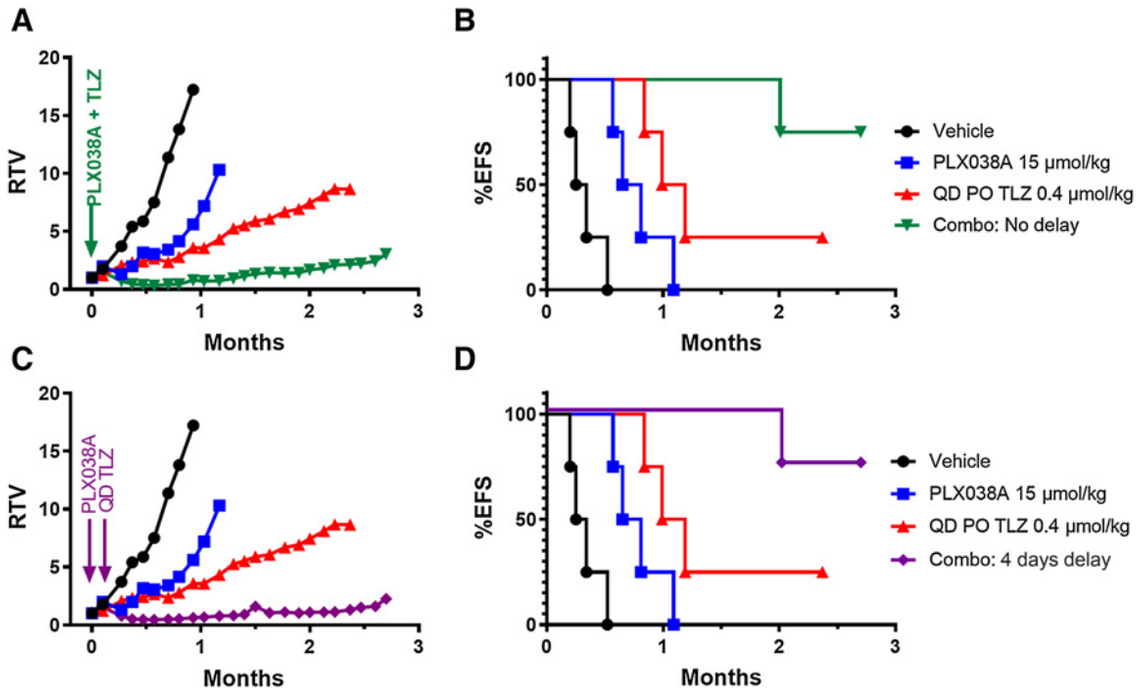

Figure 1.

Antitumor effects of combinations of PLX038A and QD PO TLZ in mice bearing TNBC MX-1 xenografts. Relative tumor volume (**A**, **C**) is plotted as the median and event-free survival (**B**, **D**) is shown using an event as a 4-fold increase in tumor volume on day 0. Xenograft bearing mice were treated with vehicle (●), a single IP dose of PL038A (■), QD PO TLZ (▲), or a combination of the two agents (▼ or ◆). Combinations were administered as a single IP dose of PLX038A on day 0 and QD PO TLZ starting on day 0 (▼; **A**, **B**) or in a gap-schedule with QD PD TLZ starting on day 4 (◆; **C**, **D**). The significance of treatments in the time to 4-fold growth in tumor size were: in **B** and **D**, vehicle vs. PLX038A or QD TLZ, and PLX038 vs. combo was $^{**}P < 0.01$. There was no statistically significant difference between the combination delivered simultaneously or with a 4-day gap.

a combination of both when administered concurrently. The interaction of a drug combination in tumor models can be semiquantitatively described by an additivity index, defined as T/C (obsd/calc), where T/C calc is the product of the T/C values of individual drugs, and T/C obsd is that of the combination. Here, an index of 1 indicates additivity and an index >1 indicates supra-additive or synergistic interactions. Using the T/C_{3wk} of PLX038A and TLZ, the calculated additive effect was 0.038, whereas the observed T/C_{3wk} of the combination was 0.062, giving an additivity index of 1.6. The combination clearly shows supra-additive effects. **Figure 1C** and **D** shows results of a similar experiment except that initiation of QD TLZ dosing was made on day 4 after the single PLX038A dose. With an elimination half-life of about 20 hours (16), ∼95% of the prodrug is eliminated from the system by this time. Nevertheless, the results of the gap schedule on tumor growth are nearly identical to that of concurrent initiation of treatment with PLX038 and TLZ and gives the same additivity index. Neither schedule led to toxicity measured by weight loss, or changes in white blood cell counts (Supplementary Figs. S1 and S2). Hence, regardless of whether treatment with a combination of PLX038A and TLZ are initiated concurrently, or using a 4-day gap, there is similar synergistic efficacy of tumor growth inhibition.

We examined the efficacy of PLX038A as a single agent in an *ATM*-proficient and -deficient tumors. Like *BRCA1/2* mutations, *ATM* loss is associated with increased sensitivity to DNA damaging agents, including TOP1i. For this study we formed tumor xenografts with an isogenic pair of WT and *ATM* knockout (*ATM* KO) 22Rv1 prostate cancer cells, treated animals with a single intraperitoneal (IP) injection of PLX038A or vehicle control, and monitored tumor growth (**Fig. 2**). For both the 22Rv1WT and 22Rv1*ATM* KO tumors, we observed a dose-dependent response in relative tumor volume and EFS, with 22Rv1*ATM* KO tumors displaying exquisite sensitivity to PLX038A compared with WT with no significant change in body weight (Supplementary Fig. S3). In the untreated cohorts, the median EFS of animals with 22Rv1WT and 22Rv1*ATM* KO tumors was similar at ∼0.5 months. Doses of PLX038A up to 30 μmol/kg consistently showed 4-fold higher sensitivity of 22Rv1*ATM* KO than WT (**Fig. 2B** and **C**; Supplementary Fig. S4). At the highest dose of PLX038A tested (60 μmol/kg), the median EFS of mice bearing 22Rv1WT tumors was 1.7 months (**Fig. 2B**) with half of the tumors quadrupling their volume in 54 days, ∼4-fold increase compared with the vehicle control. In contrast, at the same dose of PLX038A, the median EFS of animals with 22Rv1ATM KO tumors (**Fig. 2D**) was >11 months, over a 22-fold increase compared with the 0.5 months EFS of vehicle control. Moreover, 22Rv1ATM KO tumors shrank to 10% to 20% of their initial volume over 3 months. Then, between 4 and 6 months, three of eight of the *ATM* mutant tumors resumed growth while the remaining five were suppressed for an additional 8 months (**Fig. 2C**), with no palpable tumors detected in 4 animals. Of the 8 mice treated at 60 μmol/kg PLX038A, 5 survived for 9 months and 3 until study termination at 11 months. Overall, from relative increases in median EFS, at 60 μmol/kg PLX038 the *ATM* KO was over 6-fold more sensitive than the isogenic *ATM* WT tumor.

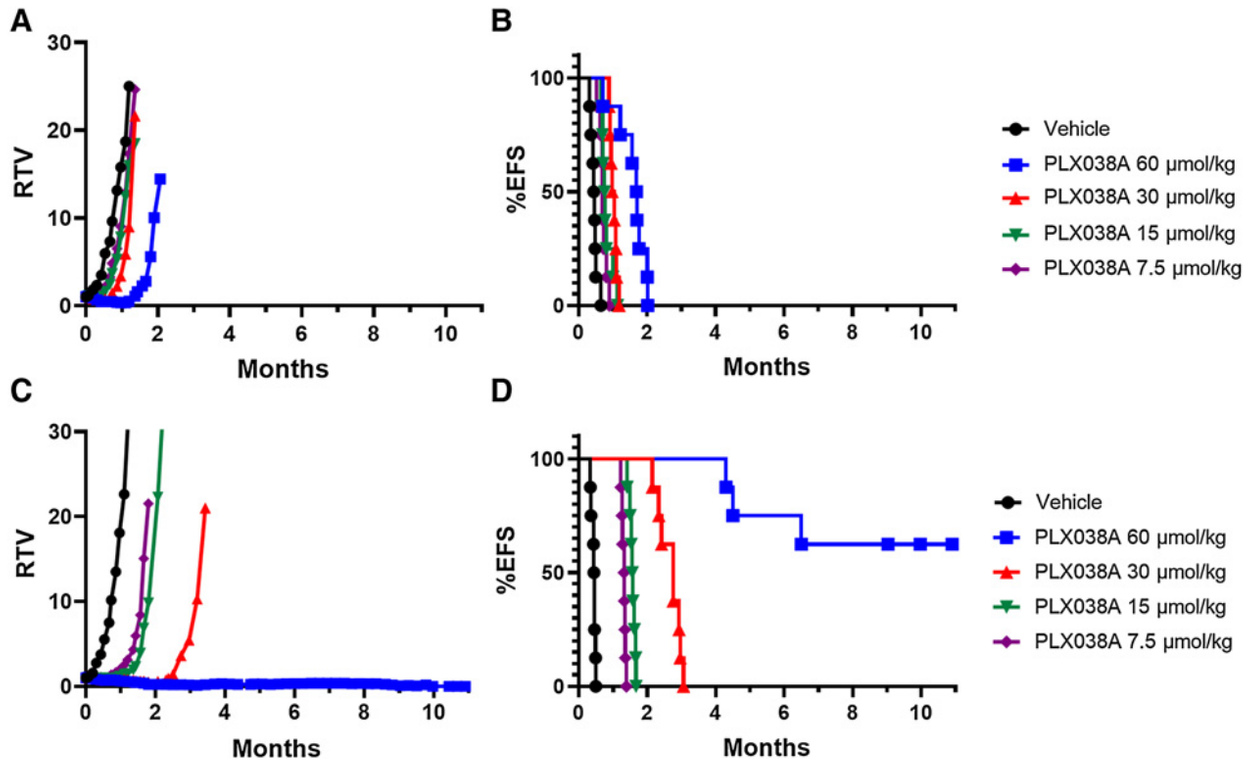

Figure 2.

Antitumor effects of PLX038A in 22Rv1WT or 22Rv1ATM KO xenografts. Mice ($N = 8$/group) bearing 22RV1 xenografts received a single IP dose of vehicle (●) or PLX038A at 7.5 (◆), 15 (▼), 30 (▲) or 60 (■) µmol/kg. **A,** Median relative tumor volume over time for mice bearing 22Rv1WT xenografts. **B,** Event-free survival for animals bearing 22Rv1WT tumors. **C,** Median relative tumor volume over time for mice bearing 22Rv1ATM KO xenografts. **D,** Event-free survival for animals bearing 22Rv1ATM KO xenografts. In **B** and **D**, an event is a 4-fold increase in tumor volume from that on day 0 of treatment. The significance of treatments in the time to 4-fold increase in tumor size were: in **B**, vehicle vs. PLX038A at 7.5- was $^{***}P < 0.001$, and 15-, 30-, and 60 µmol/kg was $^{****}P < 0.0001$. In **D**, vehicle vs. PLX038A at 7.5-, 15-, 30-, and 60 µmol/kg was $^{****}P < 0.0001$. When comparing AUC of growth curves over ∼1 month, 22Rv1ATM KO xenografts show increased sensitivity over WT at significance $^{***}P < 0.001$ for the three lower doses, and $^{*}P < 0.05$ at the highest dose.

Combinations of PLX038A and PARPi are highly synergistic in ATM-deficient tumors. **Figure 3A** shows tumor growth of 22Rv1ATM KO xenografts treated with a single low dose of 7.5 µmol/kg PLX038, daily doses of 0.4 µmol/kg TLZ, and a combination of both, and **Fig. 3B** provides the corresponding Kaplan–Meier plot showing the time for tumors to reach 4-fold their original volume. **Figure 3C** and **D** shows the same except the drug concentrations used are 50% of those in **Figure 3A** and **B**. TLZ is modestly inhibitory to growth at the higher 0.4 µmol/kg dose (**Fig. 3A**) and insignificantly inhibitory at the lower 0.2 µmol/kg dose (**Fig. 3A**). However, both combination doses—even very low doses that give little or no single-agent inhibition—cause long-term growth suppression of the 22RV1 *ATM* KO and this is clearly supra-additive over the effects calculated from the individual components. The combination of PLX038A and TLZ was tolerated and synergistic at all doses evaluated (Supplementary Fig. S5; Supplementary Table S1) and was effective at doses down to 1.9 and 0.2 µmol/kg, respectively (Supplementary Fig. S6). Indeed, the additivity index, T/C_{3wk} (obsd/calc), of 1.7 for the combination at higher doses in **Fig. 3A** is similar to the 1.6 observed in BRCA-1 deficient MX-1 tumors, but significantly higher at 3.0 for the lower dose in Fig. 3C (Supplementary Table S1). Hence, the hypersensitivity of the 22RV1 *ATM* KO towards PLX038A is not observed with single-agent TLZ, but it is clearly manifest as synergy at even very low doses of the PLX038A–PARPi combination that are barely- or non-inhibitory when administered as single agents.

Clinical trial

The demonstration of enhanced efficacy of PLX038–PARPi combination in DDR-deficient preclinical models provided compelling rationale to investigate this combination in the clinic. A patient with metastatic breast cancer and germline *ATM* mutation was enrolled in the ongoing dose escalation phase of the trial. The primary objective of the trial (Clinicaltrials.gov identifier: NCT04209595) is to identify the MTD of PLX038 in combination with PARP inhibitor rucaparib. PLX038 was administered on day 1 and rucaparib after a gap of 3 days till day 19, in 21-day cycles. The patient was initially diagnosed with locally advanced invasive ductal carcinoma and was treated with neoadjuvant chemotherapy followed by surgery and radiation. Nine years later, she developed metastatic disease expressing estrogen and progesterone receptors, and was treated with multiple anti-endocrine therapies and chemotherapies including eribulin, abraxane, and carboplatin. The patient had a strong family history of cancer including a brother who died of lung cancer at age 37, and breast cancer in a sister at age 48. At enrolment, she had skin lesions on the breast which were painful and pruritic and in addition had involvement of the lung and bones. Tumor and germline testing revealed an *ATM* p.Q1970* pathogenic mutation (c.5908C>T), located in coding exon 38. The mutation results from a C to T substitution at nucleotide position 5908 and creates a premature translational stop signal, which is expected to result in an absence or disrupted *ATM* protein. The variant was not

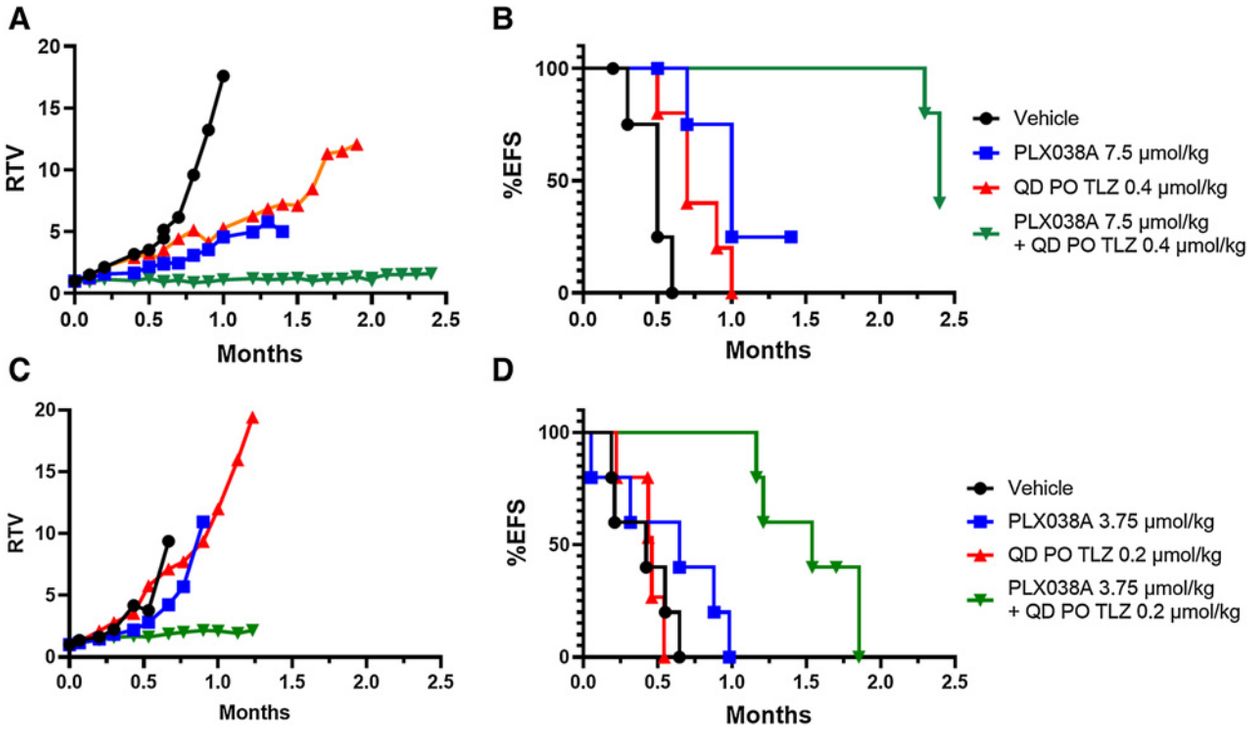

Figure 3.

Antitumor efficacy of the combination of PLX038A and TLZ in mice bearing 22Rv1ATM KO tumors. **A,** Median relative tumor volume over time of 22Rv1ATM KO xenografts. **B,** Event-free survival for 22Rv1ATM KO xenografts where an event is a 4-fold increase in tumor volume from that on day 0 of treatment. **A** and **B,** mice ($N = 5$) bearing 22RV1 xenografts were treated with vehicle (●), a single IP dose of PLX038A at 7.5 μmol/kg (■), QD PO TLZ at 0.4 μmol/kg (▲), or a combination of a single dose IP dose of PLX038A at 7.5 μmol/kg along with QD PO TLZ at 0.4 μmol/kg for the duration of the study (▼). **C** and **D,** mice ($N = 5$) xenografts were treated as above with 50% the concentrations of PLX038A and TLZ used in **A** and **B**. The significance of treatments in the time to 4-fold increase in tumor size were: in **B**, the vehicle vs. PLX038A was $^{**}P < 0.01$, vehicle vs. QD TLZ was $^{*}P < 0.05$, PLX038 vs. combo was $^{*}P < 0.05$, and TLZ vs. combo was $^{**}P < 0.01$; in **D**, combo vs. PLX038A or TLZ was $^{**}P < 0.01$.

present in population databases such as ExaC but has been reported in the literature in individuals with ataxia–telangiectasia and recognized as a founder mutation in the Costa Rican population (20).

The combination of low-dose PLX038 and rucaparib resulted in substantial reduction in this patient's tumor burden and resolution of cancer symptoms within the first cycle of treatment, qualifying as a complete response (**Fig. 4**). Shortly after initiation of treatment, the patient experienced non–dose-limiting gastrointestinal adverse effects that required reduction of the rucaparib dose and then its suspension 4 months after treatment initiation. Thereafter, the patient was treated solely with single-agent, low-dose PLX038, which resulted in sustained suppression of the tumor that lasted for a total of 12 months after treatment initiation—a result consistent with the aforementioned high sensitivity of an *ATM*-deficient xenograft to low doses of PLX038A.

Discussion

ATM is a tumor suppressor gene, which is frequently mutated in a broad range of human cancers. Although hypersensitivity of *ATM*-defective cells to DNA damage was described almost five decades ago (21), despite considerable interest in *ATM* as therapeutic target for cancer therapy, clinically effective approaches to leverage this sensitivity are lacking. Herein, we describe preclinical studies of PLX038—a releasable PEG-conjugate of TOP1i SN-38—as a potent single agent and in combination with PARPi in *BRCA1* and *ATM* mutant xenografts. We also report a complete and durable tumor response to a combination of PLX038 and PARPi rucaparib in a patient with *ATM*-deficient breast cancer.

PLX038A showed strong antitumor synergy with PARP inhibition in a BRCA1-deficient xenograft whether administered concurrently or with a 4-day gap separating administration of a single dose of PLX038 and QD PARPi. The gapped scheduling approach has been recently proposed as an approach to reduce toxic effects of combining a DNA-damaging agents and a DDRi (15). Here, the tumor-targeted PLX038A is first administered and allowed to passively accumulate in the tumor (12), followed by a gap that allows for systemic but not tumor elimination of the agent; then, during the time when PLX038A is present in the tumor but is low in normal tissues, the PARPi is administered. To our knowledge, this provides the first preclinical experimental evidence that the proposed gapped-scheduling is indeed effective. We also found that PLX038A was ∼5-fold more effective as a single agent in growth inhibition of isogenic *ATM*-deficient versus replete xenografts. When combinations of PLX038A and the PARPi were administered at doses of the individual agents that were ineffectual, there was profound synergism of combined drugs, even greater than the TOP1–PARPi combination in BRCA1-deficient tumors. It seems that PLX038A increases the vulnerability of the *ATM*-deficient tumor to low doses of the PARPi. Hence, *ATM*-deficient tumors are

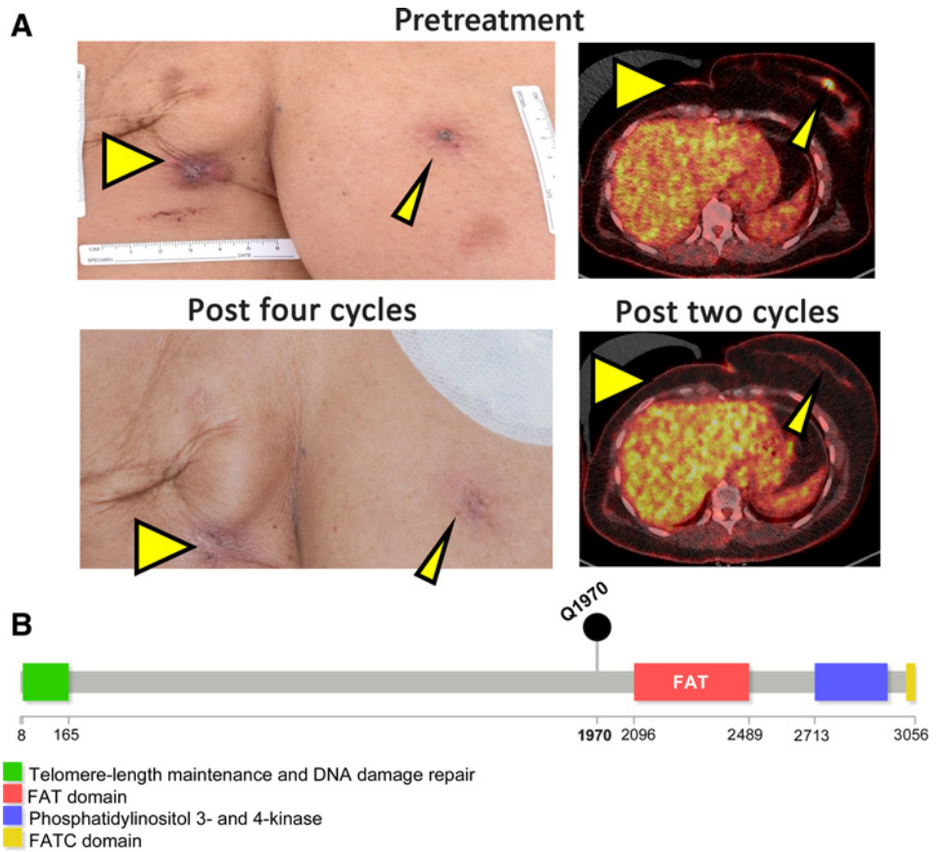

Figure 4.
Complete response to PLX038 and rucaparib combination in a patient with metastatic breast cancer with pathogenic germline *ATM* mutation. **A,** FDG-PET before and 2 months after starting treatment. The recurrent breast cancer lesion in the skin regressed completely anatomically and metabolically (yellow arrows) as well as the metastatic lesions. **B,** Lolliplot representing the mutation in the *ATM* gene.

ultrasensitive to PLX038A as a single agent, and in combination with a PARPi.

On the basis of these and other preclinical results on the synergy of TOP1i and PARPi, we initiated a clinical trial of PLX038 with rucaparib, and in the dose-escalation phase of the trial observed a remarkable response of patient with an *ATM*-deficiency. This patient showed a complete response after only the first cycle of treatment. Subsequently, because of GI adverse effects, the rucaparib dose was lowered and then suspended 4 months after treatment initiation. Thereafter, the patient was treated solely with single-agent, low-dose PLX038 which maintained the complete response for 12 months after initiation of treatment. Whether this patient's initial rapid response was due to one or both drugs is not known, but it is notable that the *ATM*-deficient preclinical model is highly susceptible to very low concentrations of the PLX038A–PARPi combination; possibly, *ATM*-deficient tumors could be effectively treated with very low doses of TOP1i–PARPi that do not cause the hematologic toxicities typically observed with a DNA-damaging agent and DDRi (15). Regardless, it is likely that PLX038 promoted maintenance of the durable complete remission because it was the sole treatment over most of the remission period. We posit that *ATM*-deficient tumors may be a sensitive target for PLX038 as a single agent or in combination with other DDRi such as a PARP or ATR inhibitors.

Identifying loss of ATM function in tumor cells might allow for the characterization of a patient subset that could receive benefit from the approach described herein. The large size of the *ATM* gene, 66 exons spanning approximately 150 kb of genomic DNA, together with the diversity and broad distribution of mutations renders routine DNA sequencing a challenging diagnostic tool (22). But cancer-associated *ATM* mutations can lead to a reduction in *ATM* protein expression and loss of *ATM* activity is often associated with reduced ATM protein levels (23). In addition to deleterious mutations, loss of ATM activity may also result from epigenetic silencing (24). Thus, ATM protein expression by IHC may be a valuable clinical tool to identify the patient subgroup spanning multiple tumor types with low or absent ATM protein levels (23). Clinical trials of PLX038 as a single agent and in combination with DNA repair inhibitors in *ATM*-deficient tumors are planned.

Authors' Disclosures

A. Thomas reports grants from EMD Serono, Astra Zeneca, Immunomedics, Prolynx, and Tarveda during the conduct of the study. S.D. Fontaine reports personal fees and other support from ProLynx during the conduct of the study; personal fees and other support from ProLynx outside the submitted work; also has a patent 10,016,411 issued to ProLynx and a patent for US20200397778A1 issued to ProLynx. A. Ashworth reports grants from Astra Zeneca and SPARC; personal fees from Tango Therapeutics, Azkarra Therapeutics, Prolynx, Ovibio, Kyttaro, Circle, Trial Library, Genentech, GSK, PhoenixMD, Ambagon, Yingli, Cambridge Science Corp, Bluestar, Earli, Cytomx, and Gladiator outside the submitted work; and also has patents on the use of PARP inhibitors held jointly with Astra Zeneca. F.Y. Feng reports personal fees from Janssen Oncology and Bayer, Myovant Sciences, Roivant Sciences, Astellas, Foundation Medicine, Varian, Bristol Myers Squibb (BMS), Exact Sciences, Novartis, and Tempus; other support from PFS Genomics, Serimmune, BlueStar Genomics, and Arteraoutside the submitted work. G.W. Ashley reports a patent for US 8,754,190 issued and a patent for US20200397778A1 pending. D.V. Santi reports personal fees and other support from ProLynx during the conduct of the study; personal fees and other support from ProLynx outside the submitted work; also has a patent for US 10,016,411 issued to ProLynx and a patent for US20200397778A1 pending to ProLynx. No disclosures were reported by the other authors.

Authors' Contributions

A. Thomas: Conceptualization, data curation, formal analysis, supervision, investigation, methodology, writing–original draft, project administration, writing–review and editing. **S.D. Fontaine:** Conceptualization, resources, data curation, formal analysis, supervision, investigation, visualization, methodology, writing–original draft, project administration, writing–review and editing. **M.E. Diolaiti:** Data curation, formal analysis, supervision, investigation, visualization, methodology, writing–original draft, project administration, writing–review and editing. **P. Desai:** Investigation. **R. Kumar:** Investigation. **N. Takahashi:** Data curation, investigation. **L. Sciuto:** Data curation, investigation. **S. Nichols:** Data curation, investigation. **A. Ashworth:** Conceptualization, formal analysis, supervision, methodology, project administration, writing–review and editing. **F.Y. Feng:** Resources. **G.W. Ashley:** Conceptualization, formal analysis, writing–original draft, writing–review and editing. **M. Nguyen:** Resources. **Y. Pommier:** Conceptualization, formal analysis, supervision, writing–review and editing. **D.V. Santi:** Conceptualization, resources, supervision, methodology, writing–original draft, project administration, writing–review and editing.

Acknowledgments

The authors gratefully acknowledge the contributions of the patients who participated in the study. This clinical work was supported by the intramural programs of the Center for Cancer Research, National Cancer Institute (ZIA BC 011793). We thank the UCSF Preclinical Therapeutics Core which is supported in part by P30CA082103.

The publication costs of this article were defrayed in part by the payment of publication fees. Therefore, and solely to indicate this fact, this article is hereby marked "advertisement" in accordance with 18 USC section 1734.

Note

Supplementary data for this article are available at Molecular Cancer Therapeutics Online (http://mct.aacrjournals.org/).

Received March 28, 2022; revised June 2, 2022; accepted August 15, 2022; published first August 23, 2022.

References

1. Knijnenburg TA, Wang L, Zimmermann MT, Chambwe N, Gao GF, Cherniack AD, et al. Genomic and molecular landscape of DNA damage repair deficiency across the cancer genome atlas. Cell Rep 2018;23:239–54.
2. Martin LP, Hamilton TC, Schilder RJ. Platinum resistance: the role of DNA repair pathways. Clin Cancer Res 2008;14:1291–5.
3. Hall MJ, Bernhisel R, Hughes E, Larson K, Rosenthal ET, Singh NA, et al. Germline pathogenic variants in the ataxia telangiectasia mutated (*ATM*) gene are associated with high and moderate risks for multiple cancers. Cancer Prev Res 2021;14:433–40.
4. Choi M, Kipps T, Kurzrock R. *ATM* mutations in cancer: therapeutic implications. Mol Cancer Ther 2016;15:1781–91.
5. Weston VJ, Oldreive CE, Skowronska A, Oscier DG, Pratt G, Dyer MJS, et al. The PARP inhibitor olaparib induces significant killing of *ATM*-deficient lymphoid tumor cells in vitro and in vivo. Blood 2010;116:4578–87.
6. Balmus G, Pilger D, Coates J, Demir M, Sczaniecka-Clift M, Barros AC, et al. *ATM* orchestrates the DNA-damage response to counter toxic non-homologous end-joining at broken replication forks. Nat Commun 2019;10:87.
7. Bang YJ, Xu RH, Chin K, Lee KW, Park SH, Rha SY, et al. Olaparib in combination with paclitaxel in patients with advanced gastric cancer who have progressed following first-line therapy (GOLD): a double-blind, randomised, placebo-controlled, phase 3 trial. Lancet Oncol 2017;18:1637–51.
8. Marshall CH, Sokolova AO, McNatty AL, Cheng HH, Eisenberger MA, Bryce AH, et al. Differential response to olaparib treatment among men with metastatic castration-resistant prostate cancer harboring BRCA1 or BRCA2 versus *ATM* mutations. Eur Urol 2019;76:452–8.
9. Pommier Y. DNA topoisomerase I inhibitors: chemistry, biology, and interfacial inhibition. Chem Rev 2009;109:2894–902.
10. Dhawan MS, Rahimi R, Karipineni S, Wilch L, Zigman E, Aggarwal RR, et al. Phase I study of rucaparib and irinotecan in advanced solid tumors with homologous recombination deficiency (HRD) mutations. J Clin Oncol 2020; 38:3513.
11. Santi DV, Schneider EL, Ashley GW. Macromolecular prodrug that provides the irinotecan (CPT-11) active-metabolite SN-38 with ultralong half-life, low C(max), and low glucuronide formation. J Med Chem 2014; 57:2303–14.
12. Beckford Vera DR, Fontaine SD, VanBrocklin HF, Hearn BR, Reid R, Ashley GW, et al. PET imaging of the EPR effect in tumor xenografts using small 15 nm diameter polyethylene glycols labeled with zirconium-89. Mol Cancer Ther 2020; 19:673–9.
13. Murai J, Zhang Y, Morris J, Ji J, Takeda S, Doroshow JH, et al. Rationale for poly(ADP-ribose) polymerase (PARP) inhibitors in combination therapy with camptothecins or temozolomide based on PARP trapping versus catalytic inhibition. J Pharmacol Exp Ther 2014;349:408–16.
14. Patel AG, Flatten KS, Schneider PA, Dai NT, McDonald JS, Poirier GG, et al. Enhanced killing of cancer cells by poly(ADP-ribose) polymerase inhibitors and topoisomerase I inhibitors reflects poisoning of both enzymes. J Biol Chem 2012; 287:4198–210.
15. Thomas A, Pommier Y. Targeting topoisomerase I in the era of precision medicine. Clin Cancer Res 2019;25:6581–9.
16. Fontaine SD, Hann B, Reid R, Ashley GW, Santi DV. Species-specific optimization of PEG∼SN-38 prodrug pharmacokinetics and antitumor effects in a triple-negative BRCA1-deficient xenograft. Cancer Chemother Pharmacol 2019; 84:729–38.
17. Morton CL, Houghton PJ. Establishment of human tumor xenografts in immunodeficient mice. Nat Protoc 2007;2:247–50.
18. Kaur H, Salles DC, Murali S, Hicks JL, Nguyen M, Pritchard CC, et al. Genomic and clinicopathologic characterization of *ATM*-deficient prostate cancer. Clin Cancer Res 2020;26:4869–81.
19. Ghilu S, Li Q, Fontaine SD, Santi DV, Kurmasheva RT, Zheng S, et al. Prospective use of the single⊠mouse experimental design for the evaluation of PLX038A. Cancer Chemother Pharmacol 2020;85:251–63.
20. Telatar M, Teraoka S, Wang ZJ, Chun HH, Liang T, Castellvi-Bel S, et al. Ataxia-telangiectasia: Identification and detection of founder-effect mutations in the *ATM* gene in ethnic populations. Am J Hum Genet 1998;62:86–97.
21. Taylor AM, Harnden DG, Arlett CF, Harcourt SA, Lehmann AR, Stevens S, et al. Ataxia telangiectasia: a human mutation with abnormal radiation sensitivity. Nature 1975;258:427–9.
22. Concannon P, Gatti RA. Diversity of *ATM* gene mutations detected in patients with ataxia-telangiectasia. Hum Mutat 1997;10:100–7.
23. Weber AM, Ryan AJ. *ATM* and ATR as therapeutic targets in cancer. Pharmacol Ther 2015;149:124–38.
24. Vo QN, Kim WJ, Cvitanovic L, Boudreau DA, Ginzinger DG, Brown KD. The *ATM* gene is a target for epigenetic silencing in locally advanced breast cancer. Oncogene 2004;23:9432–7.